GEOPHYSICAL RESEARCH LETTERS, VOL. 35, LXXXXX, doi:10.1029/2008GL035092, 2008

On the variability of ENSO at millennial timescales

Geli Wang[1] and Anastasios A. Tsonis[2]

Received 20 June 2008; revised 8 July 2008; accepted 17 July 2008; published XX Month 2008.

[1] We present an analysis of a proxy ENSO record spanning the last 11,000 years and we investigate its scaling properties. We find that the data exhibit positive long-term correlations (persistence) which extend to timescales up to half a millennium. This will indicate that a given ENSO state (El Nino or La Nina) may dominate the tropical Pacific for centuries. This provides new information on ENSO dynamics and its worldwide effects and opens new questions as to the kinds of mechanisms are responsible for these long-term correlations. **Citation:** Wang, G., and A. A. Tsonis (2008), On the variability of ENSO at millennial timescales, *Geophys. Res. Lett.*, *35*, LXXXXX, doi:10.1029/2008GL035092.

1. Introduction

[2] It goes without saying that the El Nino/Southern oscillation (ENSO) phenomenon is one of the major players in climate. Its effects are worldwide and often devastating. Its properties and dynamics have been studied extensively using both models and observations. However, while models may point to interesting insights about ENSO variability over long timescales [see, e.g., *Clement et al.*, 2000], observations are too limited to address this issue and thus to confirm model results. As such ENSO variability over millennia timescales is not well understood. Recently, proxy ENSO records have been constructed [*Rodbell et al.*, 1999; *Moy et al.*, 2002] thus providing an opportunity to study this variability. Here we consider the *Moy et al.* [2002] proxy record to study the scaling properties of ENSO over the last 11,000 years. This record (Figure 1) is based on the distribution of inorganic clastic laminae in a core retrieved from Lake Laguna Pallcacocha in Ecuador. As explained by *Moy et al.* [2002] during warm ENSO events convective precipitation along the coastal regions of north-western South America erodes the landscape and initiates debris-flow activity within the drainage basin. This activity increases stream discharge and sediment load in a single stream that enters Laguna Pallcacocha thereby depositing the inorganic laminae in the sediment core extracted from the lace. These laminae are mixed with dark-coloured organic-rich silt. The surface of the core sections was scanned and the intensity of the red colour was used to generate the proxy record. Then an age model was applied to create a yearly time series of events from 11,000 calendar years BP to today.

[3] According to the record, from 11,000 BP to about 5,000 BP the normal state (La Nina; low red colour intensity) is dominant, whereas in the last 5,000 years a switch to more frequent and strong El Nino events (high red colour intensity) has taken place. *Moy et al.* [2002] suggest that this shift was due to changes in boreal summer insolation, a suggestion that is consistent with a modeling study using the Zebiak and Cane ENSO model [*Clement et al.*, 2000]. Independent of that, however, visual inspection of the record suggests (especially from 5,000 BP to present) that either state (El Nino or La Nina) may persist for centuries. Modern records suggest that ENSO's either state may persist over time scales of a few decades. For example, since the late 1970s El Nino events tend to persist, whereas from 1950 to late 1970s La Nina was persistent. The possibility that this persistence extends to scales of centuries or millennia is very intriguing. The purpose of this work is to present a modern analysis that provides answers to this question. According to this analysis the fluctuations of the detrended record are mapped onto a random walk and then the scaling properties of the walk are investigated. As explained below these properties can reveal long term correlations and persistence in the original data.

2. Methods and Results

[4] First, the mean value is subtracted from each value to produce anomalies and then any remaining long term trend is removed linearly to produce the fluctuations T'. The linear trend (if any) is removed to avoid introducing spurious persistence in the data from timescales of the order of the length of the data. Then, the T' signal is mapped onto a walk by calculating a net displacement $y(i)$ defined by the running sum [*Tsonis*, 1992; *Tsonis et al.*, 1998]:

$$y(i) \sum_{j=1}^{i} T'(j) \qquad \mathrm{i} = 1, 11000 \tag{1}$$

This running sum describes the sequence of anomalous events over time and is influenced by the magnitude and persistence of the fluctuations. Figure 2 shows the variation of the running sum (equation (1)). Note that because the evolution is from the past to present we sum from the end (11,000 BP) to present. Thus $y(1)$ is the T' value at 11,000 years BP, $y(2)$ is the sum of the T' values at 11,000 and 10,999 years BP and so on. Mapping onto a random walk is an efficient approach to represent important low-frequency variations. If climate forcings in a period Δt are such that positive (negative) fluctuations are more frequent than negative (positive) fluctuations, the corresponding running sum exhibits a positive (negative) slope in that time interval. Therefore, time variations in the running sum are important indications of regime changes.

[1]Institute of Atmospheric Physics, Chinese Academy of Sciences, Beijing, China.
[2]Program in Atmospheric Sciences, Department of Mathematical Sciences, University of Wisconsin-Milwaukee, Milwaukee, Wisconsin, USA.

0094-8276/08/2008GL035092$05.00

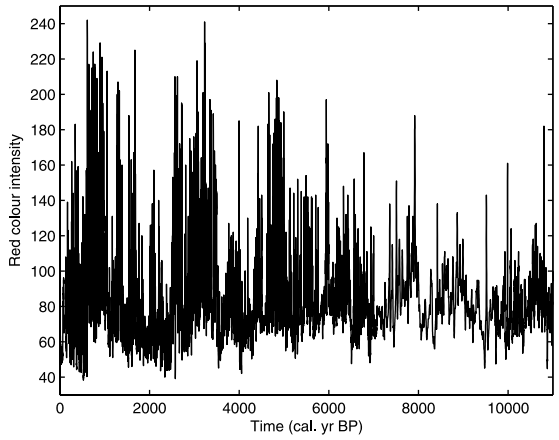

Figure 1. The proxy ENSO record of *Moy et al.* [2002] used in this study.

[5] An appropriate statistical quantity used to characterize the walk is the root mean square fluctuation about the average displacement [*Montroll and Shlesinger*, 1984; *Peng et al.*, 1992; *Buldyrev et al.*, 1995; *Tsonis et al.*, 1998]:

$$F(t) = \left[\langle[\Delta y(t)]^2\rangle - \langle[\Delta y(t)]\rangle^2\right]^{1/2} \quad (2)$$

where $\Delta y(t) = y(i+t) - y(i)$, and the symbols (< >) indicate average over all positions i of the walk. Operationally, this is equivalent to the following steps: (1) consider a caliper of distance (time scale) $t = 1$, (2) start from the beginning position ($i = 1$) and calculate $\Delta y(1)$ for $i = 1$, (3) move to the second position ($i = 2$) and calculate $\Delta y(1)$ for $i = 2$ and so on, (4) average over all positions the quantities in equation (2) to obtain $F(t)$ for $t = 1$, (5) repeat for other time scales. Note that in equation (2) $F^2(t)$is nothing else than the variance of the increments $\Delta y(t)$.

[6] It has by now clearly established that if $F(t)$ scales according to $F(t) \sim t^H$ ($0 < H < 1$), then the exponent H (otherwise known as the Hausdorff exponent) estimated from the variance of the *running sum y(i)*, implies the following conditions for the *original* signal $T'(i)$ [*Mandelbrot*, 1983; *Feder*, 1988; *Malamud and Turcotte*, 1999; *Carvalho et al.*, 2007]:

$$\begin{aligned} &\text{If } H < 0.5, \text{then } T'(i) \text{exhibits anti}-\text{persistence} \\ &\text{If } H = 0.5, \text{then } T'(i) \text{ is a sequence of uncorrelated values} \\ &\text{If } 0.5 < H < 1, \text{then } T'(i) \text{ exhibits persistence} \end{aligned} \quad (3)$$

where persistence means that chances are that a present tendency in the data will continue in the future and anti-persistence means that chances are that a present tendency in the data will be reversed in the future. A walk with $H = 0.5$ corresponds to pure Brownian motion. A walk with $H \neq 0.5$ is called a fractional Brownian motion (fBm). Note that both spectral analysis on $T'(i)$ and fluctuation analysis on $y(i)$ provide the same information since if $F(t) \sim t^H$ then $2H + 1 = \beta$, where β is the scaling exponent in the spectral density $S(f) \sim f^{-\beta}$ [*Peitgen and Saupe*, 1988; *Carvalho et al.*, 2007]. The advantage of using the running sum approach is that it provides a more efficient way to estimate H than spectral analysis does for β. Direct estimation of β is difficult because noise inherent to the spectral density of $T'(i)$ masks the presence of scaling regimes. On the other hand $F(t)$ is a much smoother function of t, and H is obtained more precisely. The reason is that the root mean square fluctuation is related to the autocorrelation function $C(t) = \langle T'(i)T'(i+t)\rangle - \langle T'(i)\rangle^2$ according to the relation $F^2(t) = \sum_{i=1}^{t}\sum_{j=1}^{t} C(j-i)$ [*Stanley*, 1971]. Because F is related to C through a double sum, fluctuations in F are substantially reduced compared to fluctuations in C (which relates to spectral density). We should stress here that persistence is not the same as periodicity. Persistence is a symmetry property akin to fractal structures incorporating intrinsic variability and transitions at all scales over which it holds and is often the result of nonlinear dynamics. A periodic signal's spectral density does not scale as $S(f) \sim f^{-\beta}$ and therefore in this case H is meaningless. Thus, while spectral methods such as the wavelet analysis of *Moy et al.* [2002] or low-pass filters (Figure S1[1]) may provide information about the nature of oscillation in the data they cannot address the issue of persistence.

[7] Figure 3 shows $lnF(t)$ versus lnt for the displacement in Figure 2. We observe a rather clear linear regime up to timescales of about of 400 years ($lnt = 6$) and a subsequent slow "leveling off" resulting from poor statistics as the timescale approaches the length of the data. The slope of the linear fit in the range $0 \leq lnt \leq 6$ is 0.85 ± 0.03. This result will indicate that the original data exhibit positive long-range correlations and persistence over timescales of several centuries. This is an important result indicating that either ENSO state can persist (or dominate) over the tropical Pacific for centuries. In the past, inferring scaling properties from double logarithmic plots such as Figure 3 has been criticized as not rigorous [*Tsonis and Elsner*, 1995] for the reason that in these plots everything may appear linear due to suppressing properties of logarithms. It has subsequently been suggested that identifying scaling regions should be done by looking for plateaus in the first derivative of the $lnF(t)$ function (or the local slope as a function of time) [*Tsonis*, 1992; *Tsonis and Elsner*, 1995; *Tsonis*, 1998] together with a comparison with appropriate surrogate data. The idea is that if a displacement is claimed to be an fBm with a given H, then it should be compared to surrogate data generated from the family of fBms with that H. Generating fBms with a desired H is now very easy and effective. For example, Figure 4 shows two simulations of an fBm with $H = 0.85$ using the algorithm of *Lowen* [1999]. Visually these records show many qualitative similarities with Figure 2. This provides the means to test the statistical significance of an alleged scaling. In Figure 5 the dashed line shows the local slope of the function in Figure 3 as a function of time. In the same graph we show the mean local slope (middle solid line) from a family of 1000 fBms with $H = 0.85$. The solid lines below and above the mean show the 5–95 percentiles of the frequency distribution of H. According to this set up the alleged scaling is statistically significant as long as the dashed line falls between the upper and lower bounds. We see that indeed the scaling properties of

[1]Auxiliary materials are available in the HTML. doi:10.1029/2008GL035092.

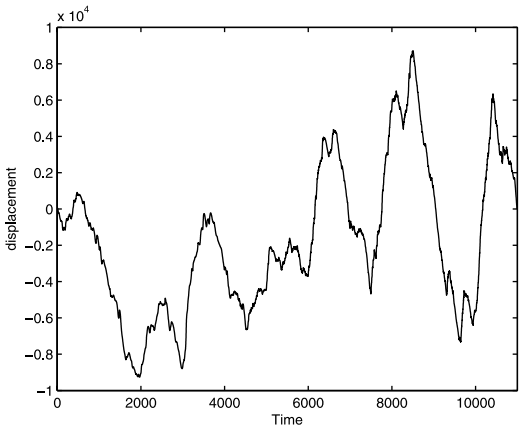

Figure 2. The net displacement (equation (1)) of a random walk produced by mapping the detrended fluctuations of the record in Figure 1. The displacement has units of red colour intensity.

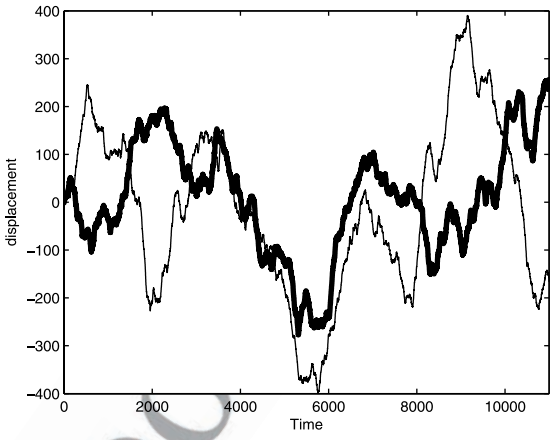

Figure 4. Two examples of simulated fractional Brownian motions with $H = 0.85$ using the algorithm of *Lowen* [1999]. The simulations show similar qualitative features to those in Figure 2.

Figure 2 are consistent with those of the family of fBms with $H = 0.85$ for time scales up to about 500 years.

[8] Thus, we establish that the original data of red colour intensity exhibit positive long-range correlations extending to timescales of half a millennium. Note that the above analysis does not necessarily imply that the best fit is $H = 0.85$. It gives the probability that the data are consistent with a family of fBms with $H = 0.85$. Whether the best fit is $H = 0.85$ or something close to that does not affect the conclusion of persistence. Figure S2 is a comparison with a family of fBms with $H = 0.5$. Figure S2 clearly shows that the data up to 500 years are not consistent with uncorrelated values. We also note that in the literature, the sort of analysis performed here is often done by the alternative method Detrended Fluctuation Analysis (DFA) [*Koscielny-Bunde et al.*, 1998]. We find no significant differences between DFA and the method we used here. We have also repeated the above analysis for the segments 11,000–5,000 BP and 5,000 BP-present. As mentioned earlier according to *Moy et al.* [2002], a shift in the dynamics appears to have taken place some time around 5,000 BP. Whether this shift was the result of some variable forcing is debatable as model runs have shown that long timescale ENSO variations may also occur without the need of a variable forcing [*Cane and Clement*, 1999]. We find that the persistence with $H \approx 0.85$ observed in the overall record is present in the two separate segments as well. Since it is doubtful that the process of constructing the proxy record will artificially produce long-range correlations, this will indicate that this property is independent of the apparent change in dynamic behavior around 5,000 BP and is a robust intrinsic property of the ENSO system, possibly due to long-term ocean memory. It

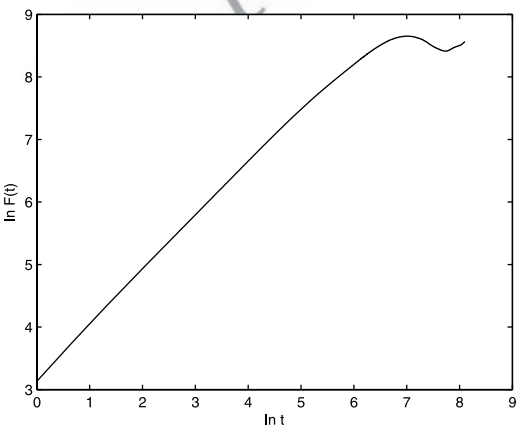

Figure 3. The root mean square fluctuation about the average displacement, $F(t)$, as a function of time in a double logarithmic plot. A linear regime with a slope of about 0.85 is visible up to $lnt = 6$ (400+ years).

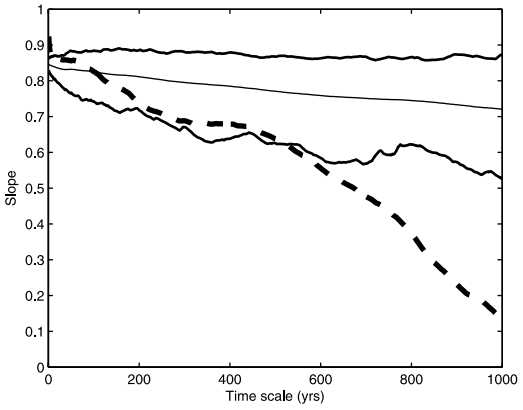

Figure 5. The derivative of the function in Figure 3 as a function of time (dashed line). The middle solid line shows the mean of the distribution of H from a family of 1000 fBms with $H = 0.85$. The solid lines below and above the mean show the 5–95 percentiles of the frequency distribution of H. The alleged scaling in Figure 3 is statistically significant as long as the dashed line falls between the lower and upper bounds. This Figure indicates that indeed the scaling properties of the original data are consistent with those of the family of fBms with $H = 0.85$ for time scales up to about 500 years.

will be interesting to see if model runs exhibit the persistence property as well.

3. Conclusions

[9] Our results provide insights about the dynamics of ENSO and open new questions as to what kinds of mechanisms are responsible for such variability. Given the well known effects of El Nino and La Nina over many areas of the globe understanding this long-term variability is crucial in preparing for long lasting extremes. In the past such long lasting extremes may have had serious consequences for many cultures. For example, it is suggested that persisting El Nino events during the period of 3,500–3,000 years BP may have contributed to the demise of the Minoan civilization. This civilization flourished from approximately 4,700 to 3,450 BP in the island of Crete, Greece, an area affected by droughts during El Nino events (M. Rosenmeier et al., unpublished manuscript, 2008).

[10] **Acknowledgment.** G.W. is supported by NSFC 40505018.

References

Buldyrev, S. V., A. L. Goldberger, S. Havlin, R. N. Mantegna, M. E. Matsa, C.-K. Peng, M. Simons, and H. E. Stanley (1995), Long-range correlation properties of coding and noncoding DNA sequences: GenBank analysis, *Phys. Rev. E*, *51*, 5084–5091.

Cane, M. A., and A. C. Clement (1999), A role for the tropical Pacific coupled ocean-atmosphere system on Milankovitch and millennial timescales part II: Global impacts, in *Mechanisms of Global Change at Millennial Time Scales, Geophys. Monogr. Ser.*, vol. 112, edited by P. U. Clark, R. S. Webb, and L. D. Keigwin, pp. 373–383, AGU, Washington, D. C.

Carvalho, L. M. V., A. A. Tsonis, C. Jones, H. R. Costa, and P. S. Polito (2007), Anti-persistence in the global temperature anomaly field, *Nonlinear Processes Geophys.*, *14*, 723–733.

Clement, A. C., R. Seager, and M. A. Cane (2000), Suppression of El Niño during the mid-Holocene by changes in the Earth's orbit, *Paleoceanography*, *15*, 731–737.

Feder, J. (1988), *Fractals*, Plenum, New York.

Koscielny-Bunde, H., A. Bunde, S. Havlin, H. E. Roman, Y. Goldreich, and J. H.-Schellnhuber (1998), Indication of a universal persistence law governing atmospheric variability, *Phys. Rev. Lett.*, *81*(3), 729–732.

Lowen, S. B. (1999), Efficient generation of fractional Brownian motion for simulation of infrared focal-plane array calibration drift, *Methodol. Comput. Appl. Probab.*, *1*(4), 445–456.

Malamud, B. D., and D. L. Turcotte (1999), Self-affine time series: I, *Generation and analyses, Adv. Geophys.*, *40*, 1–90.

Mandelbrot, B. B. (1983), *The Fractal Geometry of Nature*, W. H. Freeman, New York.

Montroll, E. W., and M. F. Shlesinger (1984), *Nonequilibrium Phenomena II: From Stochastics to Hydrodynamics, Stud. Stat. Mech.,* vol. 11, edited by J. L. Lebowitz and E. W. Montroll, North-Holland, Amsterdam.

Moy, C. M., G. O. Seltzer, D. T. Rodbell, and D. M. Anderson (2002), Variability of El Niño/Southern Oscillation activity at millennial timescales during the Holocene epoch, *Nature*, *420*, 162–165.

Peitgen, H.-O., and D. Saupe (1988), *The Science of Fractal Images*, Springer, New York.

Peng, C.-K., S. V. Buldyrev, A. L. Goldberger, S. Havlin, F. Sciortino, M. Simons, and H. E. Stanley (1992), Long-range correlations in nucleotide sequences, *Nature*, *356*, 168–170.

Rodbell, D. T., et al. (1999), An ~15000-year record of El Niño-driven alluviation in southwestern Ecuador, *Science*, *291*, 516–520.

Stanley, H. E. (1971), *Introduction to Phase Transitions and Critical Phenomena*, Oxford Univ. Press, London.

Tsonis, A. A. (1992), *Chaos From Theory to Applications*, Plenum, New York.

Tsonis, A. A. (1998), Fractality in nature, *Science*, *279*, 1611.

Tsonis, A. A., and J. B. Elsner (1995), Testing for scaling in natural forms and observables, *J. Stat. Phys.*, *81*, 869–880.

Tsonis, A. A., P. J. Roebber, and J. B. Elsner (1998), A characteristic time scale in the global temperature record, *Geophys. Res. Lett.*, *25*, 2821–2823.

A. A. Tsonis, Program in Atmospheric Sciences, Department of Mathematical Sciences, University of Wisconsin-Milwaukee, Milwaukee, WI 53201, USA. (aatsonis@uwm.edu)

G. Wang, Institute of Atmospheric Physics, Chinese Academy of Sciences, Beijing 100029, China.